Modeling Molecular Communication Channel in the Biological Sphere with Arbitrary Homogeneous Boundary Conditions

Mohammad Zoofaghari, Ali Etemadi, Hamidreza Arjmandi, Ilangko Balasingham, *Senior Member, IEEE*

***Abstract*—Diffusion-based molecular communication (DMC) is envisioned to realize nanonetworks for health applications. Inspired by sphere-like entities in the body, modeling diffusion channel in the biological sphere is motivated. The boundary condition in such biological environments is considered as homogeneous boundary conditions (HBC) that can simply model the molecular processes over biological barriers, e.g., carrier-mediated transport and transcytosis over the blood vessel walls. In this paper, we model the diffusive communication channel between a point source transmitter and a transparent receiver arbitrarily located inside a spherical environment with HBC. To this end, the concentration Green's function (CGF) is analytically derived in the Fourier domain. Statistics of the signal received at the receiver is computed based on the derived CGF to obtain the analytical results. The analytical results are accurately confirmed with particle-based simulation (PBS). The performance of a simple on-off keying modulation scheme is also examined in terms of error probability.**

***Index Terms*—Diffusive molecular communication, Green's function, Fourier transform, error probability.**

I. Introduction

Diffusion-based molecular communication (DMC) has recently received high attention to develop future embedded internet of bio-nanothing (IoBNT) devices for healthcare applications [1]-[2]. In the biological environments, DMC system has to overcome the Brownian motion and chemical reactions of the particles to convey the information [3]. The communication channel modeling in different biological environments is a vital step towards the development of DMC systems [4]. The geometry, interaction of particles with the biological barriers and corresponding boundary conditions in the environment should be taken into account in the channel modeling.

For the symmetric simple geometries, analytical channel models may be derived. As a very important symmetric geometry, spherical biological environment is inspired by sphere-like entities in the body, e.g., stomach, lung, kidney, cells, and nucleus [5]-[6]. Tumor microenvironment that is referred to as tumor spheroid can also be approximated by a spherical environment in which the outer cells make the reactive boundary [7]. This boundary behaves as a reversible binding surface for ordinary signaling molecules transmitted by the cells [7]. Moreover, the space with reactive surface in the proximity of a synaptic cleft in the presynaptic neuron where the vesicles are generated and diffuse can be considered as a sphere-like biological environment [8]. In synthetic drug-delivery systems, mathematical models are desired to describe the release rate of the particles out of the nanocarrier spheroids where the internal reactive surface characterizes the permeability rate of the membrane [9]. Modeling the release of exosomes in the vicinity of a biological barrier, e.g. spherical membrane of a cell with specific boundary conditions is another example motivating the spherical biological environment [10].

The boundary conditions in such biological environments can be simply modeled by homogeneous boundary conditions (HBC) framework proposed recently in [11]. The general HBC framework is able to model the interaction of different active transport mechanisms across the biological barriers. Considering the general HBCs for objects, transceivers, and borders in an environment with arbitrary geometries, a semi-analytical approach has been recently proposed to model the pure diffusion channel [12].

DMC literature have already addressed the channel modeling problem for molecular communication in the sphere with various simple BCs [5]-[6], [13]-[15]. Authors in [13] proposed a semi-analytical transfer function approach which models particle diffusion inside a single or across multiple conjugating spheres with variable permeability based on an initial-boundary value problem. Authors in [6] obtained analytical concentration Green's function (CGF) for a DMC system confined in a spherical environment with irreversible reaction across the boundary assuming a fully-absorbing receiver located at the origin. Furthermore, analytical CGF for the sphere with fully reflective or absorbing boundary is provided in [14]. The authors in [15] provide analytical CGF inside a sphere considering fully-reflective boundary in the presence of a spherical fully-absorbing receiver concentric with the sphere. In [5], the analytical CGF for the spherical environment with partially absorbing boundary that covers a wide range from fully-reflective to fully-absorbing BCs assuming arbitrarily-located point transmitter and transparent receiver inside the sphere. All the previous approaches are unable to consider arbitrarily-located transmitter inside a sphere with a general HBC that linearly simplifies the BC corresponding to any reaction over the boundary, e.g., reversible reactions and active transport mechanisms.

In this paper, we consider a spherical environment where the interaction of information particles with the internal surface of the sphere is generally modeled as HBC. The proposed analysis provides the CGF at any point inside the sphere assuming an arbitrarily-located point transmitter. Applying

M. Zoofaghari and H. Arjmandi are with the Department of Electrical Engineering, Yazd University, Yazd 89195-741, Iran.

A. Etemadi is with the School of Electrical and Computer Engineering, Tarbiat Modares University, Tehran 14115-111, Iran.

I. Balasingham is with the Intervention Center, Oslo University Hospital (OUS), 0372 Oslo, Norway, and also with the Department of Electronics and Telecommunications, Norwegian University of Science and Technology (NTNU), 7491 Trondheim, Norway.

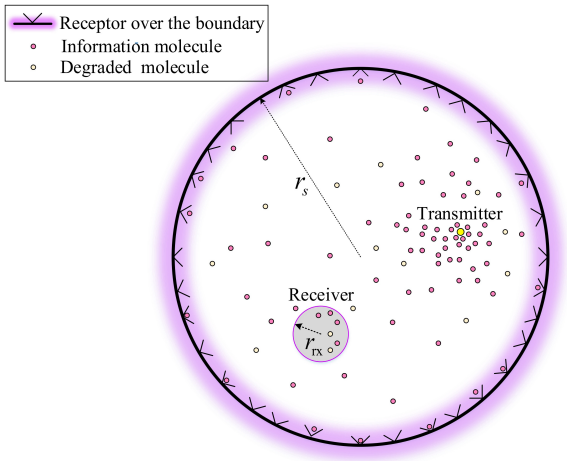

Figure 1: Schematic illustration of the considered DMC system. The point transmitter (in yellow color) and the transparent receiver (gray sphere with radius $r_{\rm rx}$) are located inside the biological sphere with radius r_s.

a frequency-domain approach, the CGF inside and over the surface of the sphere can be analytically obtained given the HBC, assuming a point transmitter and a transparent receiver. The derived Fourier transform of the CGF can be employed for important analysis in the communication systems, e.g., frequency-domain equalization, channel estimation, channel shortening, and pulse shaping from the frequency-domain perspective [16]-[17]. However, the proposed CGF may feed the sequential method of moments provided by [12] as the initial analytical CGF to get the CGF inside the sphere in the presence of multiple volumetric transceivers and/or obstacles with arbitrary HBCs.

The organization of the letter is described as follows. In Section II, the considered system model is introduced. The CGF for the described system model is derived in frequency domain in Section III. Finally, in Section IV, the provided method is evaluated by a particle-based simulation (PBS) and the corresponding bit error rate (BER) analysis are carried out for various scenarios. The paper is concluded in Section V.

II. System Model

We consider a DMC system inside a spherical boundary with radius r_s where a general HBC is conducted; see Fig. 1. The point transmitter (Tx) uses information molecules of type A to communicate with the transparent receiver (Rx). The information molecules, released by the Tx, undergo Brownian motion and some of them may reach the Rx. The spherical coordinate system (r, θ, ϕ) is adopted where r, θ, and ϕ denote the radial, elevation, and azimuthal coordinates, respectively. Also, homogeneous diffusion coefficient D is considered for diffusion of information molecules in the environment. The first order degradation reaction

$$A \xrightarrow{k_d} \emptyset \tag{1}$$

is assumed inside the sphere where k_d is the degradation constant in s^{-1}. The internal boundary of the sphere is assumed to be modeled as a general HBC [11] described as follows

$$\mathbf{D}\nabla c(\bar{r}, t) \cdot \hat{n} = \mathbf{L}c(\bar{r}, t), \quad \bar{r} \in \partial\mathcal{D}, \tag{2}$$

where ∇ denotes the spatial gradient operator, $(\cdot)$ is the inner multiplication operator, $\hat{n}$ describes the surface normal vector pointing towards the exterior of the diffusion environment at $\bar{r} \in \partial\mathcal{D}$ with $\partial\mathcal{D}$ denoting the set of all points over the boundary of the environment, $\mathbf{D}$ and $\mathbf{L}$ are arbitrary time domain differential operators which are characterized based on the reactions involving information molecules across the boundary, and $c(\bar{r}, t)$ denotes the concentration of information molecules at point $\bar{r}$ and time t. The HBC models wide range of BCs from partially absorbing BCs [5] to active transport mechanism [11] across the biological barriers, e.g., carrier-mediated transport and transcytosis [18]. Active mechanisms incorporating several reversible reactions are responsible for transport of the macromolecules across the boundary cells. For instance, a simplified model for the carrier-mediated transport across the endothelial cells is given by [11]

$$A + B \underset{k_b}{\overset{k_f}{\rightleftharpoons}} AB \xrightarrow{k_i} \emptyset \tag{3}$$

where k_f, k_b, and k_i denote forward and backward reaction constants, and molecule internalization rate, respectively. The reaction (3) reduces to the reversible reaction for $k_i = 0$ [11], i.e.,

$$D(\frac{\partial}{\partial t} + k_b)\nabla c(\bar{r}, t) \cdot \hat{n} = k_f \frac{\partial}{\partial t} c(\bar{r}, t). \tag{4}$$

In the communication setup, a simple on-off keying modulation scheme is considered. In each time slot of duration T_s, the Poisson concentration transmitter [19] encodes information bits 0 and 1 into the release of zero and N molecules on average, respectively, at the beginning of the time slot. In other words, the number of molecules released at the beginning of each time slot is modeled as a Poisson distribution with rate $b_i N$ where b_i denotes the ith bit, $i \in \{0, 1\}$ [19]-[20]. The receiver decodes the received signal based on the number of observed molecules inside the volume of the receiver measured at the peak sampling time.

III. Derivation of CGF in Frequency Domain

In this letter, a frequency domain approach is utilized to find the CGF inside the sphere, given the general HBC in (2).

The point transmitter is located at $\bar{r}_{\rm tx} = (r_{\rm tx}, \theta_{\rm tx}, \varphi_{\rm tx})$. The partial differential equation governing the diffusion process in the frequency domain and the spherical coordinate system is given by (5) [21] at the top of the next page where C is the abbreviation for $C(\bar{r}, \omega|\bar{r}_{\rm tx})$ that denotes the concentration of molecules at point $\bar{r}$ and frequency ω given the impulsive point source at $\bar{r}_{\rm tx}$ i.e. $\frac{\delta(r-r_{\rm tx})\delta(\theta-\theta_{\rm tx})\delta(\varphi-\varphi_{\rm tx})}{r^2 \sin\theta}$. HBC (2) in the spherical coordinate system and the frequency domain is obtained as

$$\mathbf{D}(\omega)\frac{\partial C(\bar{r}, \omega|\bar{r}_{\rm tx})}{\partial r}\bigg|_{\bar{r}=r_s\hat{r}} = \mathbf{L}(\omega)C(r_s\hat{r}, \omega|\bar{r}_{\rm tx}), \tag{6}$$

$$\frac{D}{r^2}\frac{\partial}{\partial r}(r^2\frac{\partial C}{\partial r})+\frac{D}{r^2\sin\theta}\frac{\partial}{\partial\theta}(\sin\theta\frac{\partial C}{\partial\theta})+\frac{D}{r^2\sin^2\theta}\frac{\partial^2 C}{\partial\varphi^2}-(k_d+i\omega)C+\frac{\delta(r-r_{\rm tx})\delta(\theta-\theta_{\rm tx})\delta(\varphi-\varphi_{\rm tx})}{r^2\sin\theta}=0 \quad (5)$$

where $\hat{r}$ is the radial unit vector. The series-form separated solution of (5) is written as [5]

$$C(r,\theta,\varphi,\omega|\bar{r}_{\rm tx}) = \sum_{n=0}^{\infty}\sum_{m=0}^{n} H_{mn}R_n(r,\omega)\cos(m(\varphi-\varphi_{\rm tx}))P_n^m(\cos\theta), \quad (7)$$

where $R_n(r,\omega)$ is unknown radial function of r, $\mathcal{F}(\theta,\varphi)=\cos(m\varphi)P_n^m(\cos\theta)$ is the associated Fourier-Legendre function of the first kind with degree n and order m that satisfies the partial differential equation (PDE) in (9), and H_{mn} denotes the unknown coefficient corresponding to the mode mn of the response. Also, the representation of $\delta(\varphi-\varphi_{\rm tx})\frac{\delta(\theta-\theta_{\rm tx})}{\sin\theta}$ based on the aforementioned Fourier-Legendre basis functions is given by (8) at the top of the current page where $L_0=\frac{1}{2\pi}$ and $L_m=\frac{1}{\pi}, m\geq 1$ [5]. Replacing C and $\delta(\varphi-\varphi_{\rm tx})\frac{\delta(\theta-\theta_{\rm tx})}{\sin\theta}$ in (5) by the corresponding series-form representation given by (7) and (8) respectively, gives (10). Matching two sides of (10) yields,

$$H_{mn}=L_m\frac{2n+1}{2}\frac{(n-m)!}{(n+m)!}P_n^m(\cos\theta_{\rm tx}), \quad (11)$$

and

$$r^2\frac{\partial^2 R_n(r,\omega)}{\partial r^2}+2r\frac{\partial R_n(r,\omega)}{\partial r}+(k^2r^2-n(n+1))R_n(r,\omega) = \delta(\bar{r}-\bar{r}_{\rm tx}), \quad (12)$$

where $k=\sqrt{\frac{-k_d-i\omega}{D}}$. By applying (7) in the HBC (6), we also obtain

$$\mathbf{D}(\omega)\frac{\partial R_n(r,\omega)}{\partial r}\Big|_{\bar{r}=(r_s,\theta,\varphi)}=\mathbf{L}(\omega)R_n(r,\omega). \quad (13)$$

To solve (12), we remove the source term $\delta(\bar{r}-\bar{r}_{\rm tx})$ in the right hand and consider the derivative discontinuity of CGF at $\bar{r}=\bar{r}_{\rm tx}$ that leads to the following corresponding boundary condition[1]

$$r^2\frac{\partial R_n(r,\omega)}{\partial r}\Big|_{r=r_{tx}^+}-r^2\frac{\partial R_n(r,\omega)}{\partial r}\Big|_{r=r_{\rm tx}^-}=1. \quad (14)$$

The solution of homogeneous form of PDE obtained from (12) is written as

$$R_n(r,\omega)=\begin{cases} A_nj_n(kr)+B_nn_n(kr) & r\geq r_{\rm tx}\\ C_nj_n(kr)+D_nj_n(kr) & r<r_{\rm tx}\end{cases} \quad (15)$$

where $j_n(.)$ and $n_n(.)$ are nth order of the first and second types of spherical Bessel function, respectively. Since $n_n(kr)$ is singular at $r=0$, we set $D_n=0$ for $r<r_{\rm tx}$. Considering the boundary conditions (13), (14), and also the continuity condition of concentration at $\bar{r}_{\rm tx}$,

$$R_n(r,\omega)\Big|_{r=r_{\rm tx}^+}=R_n(r,\omega)\Big|_{r=r_{\rm tx}^-}, \quad (16)$$

[1]The equivalent boundary condition of (14) is derived by integration of two sides of over $[r_{\rm tx}^+, r_{\rm tx}^-]$.

where coefficients A_n, B_n, and C_n in (15) are obtained as (17)-(19) at the top of the next page. Noteworthy, $j'(\cdot)$ and $n'(\cdot)$ in (17)-(19) are the derivative functions of $j(\cdot)$ and $n(\cdot)$ in terms of r, respectively. By having A_n, B_n and C_n, $R_n(r,\omega)$ is given in (15) and the concentration Green's function is computed by taking inverse Fourier transform from (7).

IV. Analytical and Simulation Results

For the results section, the spherical environment described in Section II is considered. A reversible reaction, i.e., (3) for $k_i=0$ is assumed across the boundary that corresponds to the frequency-domain HBC of (4), i.e., $\mathbf{D}(\omega)=D(i\omega+k_b)$ and $\mathbf{L}(\omega)=i\omega k_f$, respectively. The diffusion coefficient $D=10^{-9}\ \mathrm{m^2 s^{-1}}$ is assumed for information molecules. The analytical results are confirmed by the PBS [12]. Then we investigate the performance of the DMC system in terms of BER analysis.

A transparent receiver located at $\bar{r}_{\rm rx}=(4\mu\mathrm{m},\frac{\pi}{4},\frac{3\pi}{4})$ is considered in the described spherical environment with radius $r_s=5\mu\mathrm{m}$. Also, a time-slot duration $T_s=0.25$ is adopted and the receiver is assumed to have the radius $r_{\rm rx}=1\ \mu m$. The CGF at position (r,θ,ϕ) given a point transmitter located at $\bar{r}_{\rm tx}=(3\mu\mathrm{m},\frac{\pi}{2},0)$ is obtained by taking inverse Fourier transform of (7). Based on the transmitted signal model in Section II and having the analytical CGF, the discrete-time received signal at ith time slot denoted by Y_i, follows a Poisson distribution as $Y_i\sim\mathrm{Poisson}(N\mathrm{v_{rx}}\sum_{j=0}^{i}b_jc_{i-j})$ where $\{b_j\}_{j=0}^{i}$ denote the transmitted sequence up to the ith transmission time slot, i.e., $t=iT_s$, and $\mathrm{v_{rx}}=\frac{4}{3}\pi r_{\rm rx}^3$. Also, c_{i-j} is the CGF value at sampling times defined as $c_{i-j}\triangleq c(\bar{r},t)\big|_{t=(i-j)T_s+t_s}$ where t_s denotes the peak sampling time starting from the beginning of the time slot. The terms with $i\neq j$ characterize the accumulated inter-symbol interference (ISI) observed at the receiver at ith time slot.

Fig. 2 depicts the observation probability function (OPF) defined as $\mathrm{v_{rx}c(\bar{r},t)}$ which is obtained by the proposed analytical CGF and the PBS for fully reflective and fully absorbing HBCs, i.e., $k_f=0\ \mathrm{m\,s^{-1}}$, $k_f=\infty$, respectively, when different degradation constants $k_d\in\{0,20\}\ \mathrm{m\,s^{-1}}$ are adopted. The time step $\Delta t=10^{-3}$ s is assumed for the PBS. The figure also shows the results for a reversible boundary with $k_f=10^{-4}\ \mathrm{m\,s^{-1}}$ for different backward reaction constants $k_b\in\{50,10\}\ \mathrm{s^{-1}}$. As observed, the analysis is accurately confirmed by PBS. As expected, by increasing k_b, the tail of the CGF increases which results in severe ISI level and consequently higher channel memory.

Fig. 3 demonstrates the BER analysis versus time-slot duration for the DMC system for different backward reaction constants $k_b\in\{0,10,50\}\ \mathrm{s^{-1}}$ when $k_f=10^{-4}\ \mathrm{m\,s^{-1}}$ and $k_d=20\ \mathrm{s^{-1}}$. In our simulations, we have employed a symbol-by-symbol detector which determines the threshold value based on the maximum-a-posteriori rule. Due to the lack

$$\delta(\varphi-\varphi_{\rm tx})\frac{\delta(\theta-\theta_{\rm tx})}{\sin\theta}=\sum_{n=0}^{\infty}\sum_{m=0}^{n}L_m\frac{2n+1}{2}\frac{(n-m)!}{(n+m)!}P_n^m(\cos\theta)P_n^m(\cos\theta_{\rm tx})\cos\big(m(\varphi-\varphi_{\rm tx})\big), \tag{8}$$

$$\frac{D}{\sin\theta}\frac{\partial}{\partial\theta}\big(\sin\theta\frac{\partial\mathcal{F}(\theta,\varphi)}{\partial\theta}\big)+\frac{D}{\sin^2\theta}\frac{\partial^2\mathcal{F}(\theta,\varphi)}{\partial\varphi^2}+n(n+1)\mathcal{F}(\theta,\varphi)=0. \tag{9}$$

$$\begin{aligned}&\tfrac{D}{r^2}\tfrac{\partial}{\partial r}(r^2\tfrac{\partial R(r,\omega)}{\partial r})\textstyle\sum_{n=0}^{\infty}\sum_{m=0}^{n}H_{mn}P_n^m(\cos\theta)\cos(m(\varphi-\varphi_{\rm tx})+R(r,\omega)\sum_{n=0}^{\infty}\sum_{m=0}^{n}H_{mn}\tfrac{D}{r^2\sin\theta}\tfrac{\partial}{\partial\theta}(\sin\theta\tfrac{\partial P_n^m(\cos\theta)}{\partial\theta})+\\ &\tfrac{D}{r^2\sin^2\theta}\tfrac{\partial^2(\cos(m(\varphi-\varphi_{\rm tx})))}{\partial\varphi^2}-(k_d+i\omega)R(r,\omega)\textstyle\sum_{n=0}^{\infty}\sum_{m=0}^{n}H_{mn}P_n^m(\cos\theta)\cos(m(\varphi-\varphi_{\rm tx}))\\ &=-\sum_{n=0}^{\infty}\sum_{m=0}^{n}L_m\tfrac{2n+1}{2}\tfrac{(n-m)!}{(n+m)!}\times P_n^m(\cos\theta)P_n^m(\cos\theta_{\rm tx})\cos(m(\varphi-\varphi_{\rm tx}))\delta(\bar r-\bar r_{\rm tx}).\end{aligned} \tag{10}$$

$$A_n=\frac{1}{Dr_{\rm tx}^2k\left(j_n'(kr_{\rm tx})+\frac{\frac{\mathbf{L}(\omega)}{\mathbf{D}(\omega)}j_n(ka)-kj_n'(ka)}{-\frac{\mathbf{L}(\omega)}{\mathbf{D}(\omega)}n_n(ka)+kn_n'(ka)}n_n'(kr_{\rm tx})-\frac{j_n(kr_{\rm tx})+n_n(kr_{\rm tx})}{j_n(kr_{\rm tx})}j_n'(kr_{\rm tx})\right)}, \tag{17}$$

$$B_n=A_n\frac{\frac{\mathbf{L}(\omega)}{\mathbf{D}(\omega)}j_n(ka)-kj_n'(ka)}{-\frac{\mathbf{L}(\omega)}{\mathbf{D}(\omega)}n_n(ka)+kn_n'(ka)}, \tag{18}$$

$$C_n=A_n\frac{j_n(kr_{\rm tx})+n_n(kr_{\rm tx})}{j_n(kr_{\rm tx})}. \tag{19}$$

of space, the BER analysis is omitted here and is referred to our previous work [5] for the interested audience.

Fig. 4 demonstrates the normalized cumulative time error (CTE) as well as expected run time (ERT) to compute the series in (7) given a limited number of the series. The normalized CTE, denoted by $\mathcal{E}(\bar r,n)$, describes the summation of differential error in consecutive time instances and is defined as follows:

$$\mathcal{E}(\bar r,n)=\frac{\int_0^{t_{\max}}|c_n(\bar r,t)-c_{n-1}(\bar r,t)|dt}{|\int_0^{t_{\max}}c_n(\bar r,t)dt|}, \tag{20}$$

where $c_n(\bar r,t)$ denotes the channel impulse response employing n terms of series (7) where $\lim_{n\to\infty}c_n(\bar r,t)=c(\bar r,t)$, $|\cdot|$ denotes the absolute value, and $t_{\max}=0.1$ s is assumed. We consider $k_b=10\ \mathrm{s}^{-1}$, $k_f=10^{-4}\ \mathrm{m\,s}^{-1}$, and $k_d=20\ \mathrm{s}^{-1}$. We observe that CTE is enough small for $n<40$ that correspond with an ERT <30 min. The figure also shows that normalized CTE increases for larger r_s.

V. Conclusion

We have adopted a frequency-domain approach to provide an analytical CGF inside and over the boundary of the sphere with a reactive surface modeled as HBC. The HBC framework simply models BC corresponding with the reactions across the boundary, e.g., active transport mechanisms. The proposed method extends the limited time-domain approach proposed previously in [5] to consider general HBCs at the cost of a higher computational complexity of the inverse Fourier transform. The results demonstrated that the increment in backward reaction rates leads to significant performance deterioration in terms of BER due to the higher channel memory and consequently increased level of ISI. The provided framework constitutes an analytical basis of the diffusion processes inside

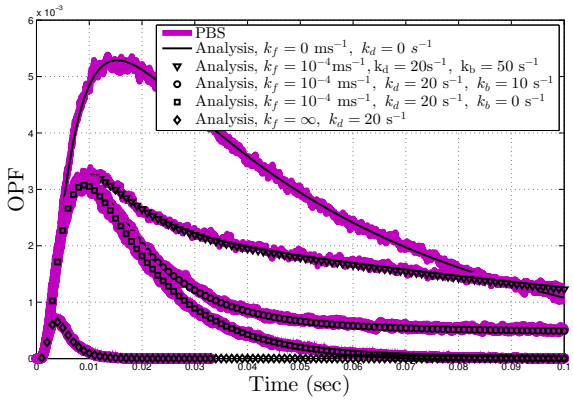

Figure 2: OPF for different values of $k_f, k_b,$ and k_d.

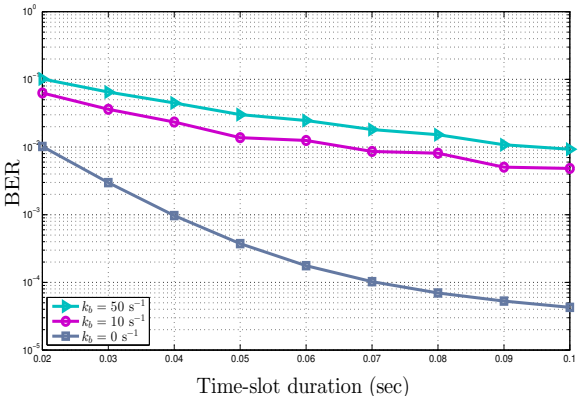

Figure 3: BER versus time-slot duration for different k_b values.

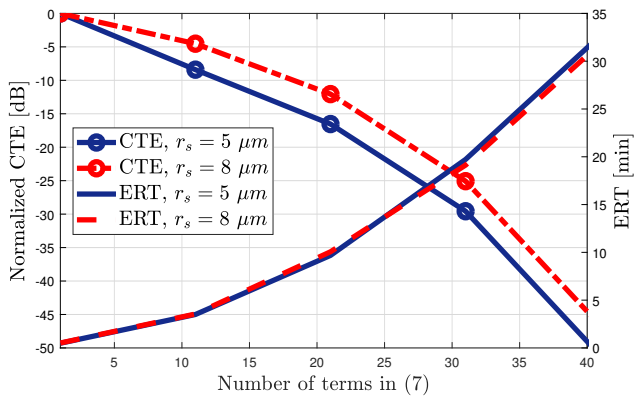

Figure 4: Normalized CTE (20) and ERT for computing the series in (7) with n terms.

sphere-like entities, paving the way for the development of realistic DMC systems, e.g., release-controlled nanocarriers. Also, the proposed analytical approach can be used to solve the inverse channel estimation problems in spherical diffusion environments which is motivated as a future work.

REFERENCES

[1] I. F. Akyildiz, M. Pierobon, S. Balasubramaniam and Y. Koucheryavy, "The internet of Bio-Nano things," in *IEEE Communications Magazine*, vol. 53, no. 3, pp. 32-40, March 2015.

[2] B. Atakan, O. B. Akan, and S. Balasubramaniam, "Body area nanonetworks with molecular communications in nanomedicine," *IEEE Communications Magazine*, vol. 50, no. 1, pp. 28-34, Jan. 2012.

[3] T. Nakano, A. W. Eckford, and T. Haraguchi, *Molecular Communication*, Cambridge, U.K.: Cambridge University Press, 2013.

[4] V. Jamali, A. Ahmadzadeh, W. Wicke, A. Noel and R. Schober, "Channel Modeling for Diffusive Molecular Communication—A Tutorial Review," in *Proceedings of the IEEE*, vol. 107, no. 7, pp. 1256-1301, July 2019.

[5] H. Arjmandi, M. Zoofaghari and A. Noel, "Diffusive Molecular Communication in a Biological Spherical Environment With Partially Absorbing Boundary," in *IEEE Transactions on Communications*, vol. 67, no. 10, pp. 6858-6867, Oct. 2019.

[6] M. M. Al-Zu'bi and A. S. Mohan, "Modeling of Ligand-Receptor Protein Interaction in Biodegradable Spherical Bounded Biological Micro-Environments," in *IEEE Access*, vol. 6, pp. 25007-25018, Apr. 2018.

[7] R. A. Carpenter, J. G. Kwak, S. R. Peyton, and J. Lee, "Implantable pre-metastatic niches for the study of the microenvironmental regulation of disseminated human tumour cells," vol. 2, no. 12, pp. 915-929, Dec. 2018.

[8] D. Malak and O. B. Akan, "Communication theoretical understanding of intra-body nervous nanonetworks," in *IEEE Communications Magazine*, vol. 52, no. 4, pp. 129-135, April 2014.

[9] F. M. Kashkooli, M. Soltani, and M. Souri, "Controlled anti-cancer drug release through advanced nano-drug delivery systems: Static and dynamic targeting strategies," *Journal of Controlled Release*, Aug. 2020.

[10] J. Y. Xu, G. H. Chen, and Y. J. Yang, "Exosomes: a rising star in failing hearts," *Frontiers in physiology*, vol. 8, no. 494, pp. 1-19, Jul. 2017.

[11] H. Arjmandi, M. Zoofaghari, S. V. Rouzegar, M. Veletić, and I. Balasingham, "On Mathematical Analysis of Active Drug Transport Coupled with Flow-induced Diffusion in Blood Vessels," in *IEEE Transactions on NanoBioscience*, vol. 20, no. 1, pp. 105-115, Jan. 2021.

[12] M. Zoofaghari, H. Arjmandi, A. Etemadi and I. Balasingham, "A Semi-analytical Method for Channel Modeling in Diffusion-based Molecular Communication Networks," in *IEEE Transactions on Communications*, doi: 10.1109/TCOMM.2021.3065372.

[13] M. Schäfer, W. Wicke, R. Robenstein, and R. Schober, "Spherical Diffusion Model with Semi-Permeable Boundary: A Transfer Function Approach," *ICC 2020 - 2020 IEEE International Conference on Communications (ICC)*, Dublin, Ireland, 2020, pp. 1-7.

[14] X. Bao, Y. Zhu and W. Zhang, "Channel Characteristics for Molecular Communication via Diffusion With a Spherical Boundary," in *IEEE Wireless Communications Letters*, vol. 8, no. 3, pp. 957-960, June 2019.

[15] F. Dinç, B. C. Akdeniz, A. E. Pusane, and T. Tugcu, "Impulse Response of the Molecular Diffusion Channel With a Spherical Absorbing Receiver and a Spherical Reflective Boundary," in *IEEE Transactions on Molecular, Biological and Multi-Scale Communications*, vol. 4, no. 2, pp. 118-122, June 2018.

[16] Y. Huang *et al.*, "Frequency Domain Analysis and Equalization for Molecular Communication," in *IEEE Transactions on Signal Processing*, vol. 69, pp. 1952-1967, Mar. 2021.

[17] M. Schäfer, W. Wicke, L. Brand, R. Robenstein, and R. Schober, "Transfer Function Models for Cylindrical MC Channels with Diffusion and Laminar Flow," *IEEE Transactions on Molecular, Biological and Multi-Scale Communications*, doi: 10.1109/TMBMC.2021.3061030.

[18] D. Mehta and A.B. Malik, "Signaling mechanisms regulating endothelial permeability," *Physiological reviews*, vol. 86, no. 1, pp. 279-367, Jan. 2006.

[19] A. Gohari, M. Mirmohseni, M. Nasiri-kenari, "Information Theory of Molecular Communication: Directions and Challenges," in *IEEE Transactions on Molecular, Biological and Multi-Scale Communications*, vol. 2, no. 2, pp. 120-142, Dec. 2016.

[20] H. Arjmandi, A. Gohari, M. N. Kenari, and F. Bateni, "Diffusion-Based Nanonetworking: A New Modulation Technique and Performance Analysis," in *IEEE Communications Letters*, vol. 17, no. 4, pp. 645-648, April 2013.

[21] P. Grindrod, *The theory and applications of reaction-diffusion equations: patterns and waves,* Clarendon Press, 1996.